SUPPORTING INFORMATION

Heme Dynamics and Trafficking Factors Revealed by Genetically Encoded Fluorescent Heme Sensors

David A. Hanna, Raven M. Harvey, Osiris Martinez-Guzman, Xiaojing Yuan, Bindu Chandrasekharan, Gheevarghese Raju, F. Wayne Outten, Iqbal Hamza, and Amit R. Reddi

1. Cell Lines, Culturing, and Plasmids

a.Yeast Strains, Media, and Growth Conditions. *S. cerevisiae* strains used in this study were derived from BY4741 (*MAT*a, *his3*Δ1, *leu2*Δ0, *met15*Δ0, *ura3*Δ0). *tdh1*Δ::*kan*MX4, *tdh2*Δ::*kan*MX4, and *tdh3*Δ::*kan*MX4 strains were obtained from the yeast gene deletion collection (Thermo Fisher Scientific). A *hem1*Δ::HIS3 strain was generated by deleting *HEM1* using the *hem1*::HIS3 deletion plasmid, pDH001. Yeast transformations were performed by the lithium acetate procedure (1). Strains were maintained at 30° C on either enriched yeast extract-peptone based medium supplemented with 2% glucose (YPD), or synthetic complete medium (SC) supplemented with 2% glucose and the appropriate amino acids to maintain selection. Culturing of *hem1*Δ cells required supplementing YPD or SC media with 50 µg/mL of 5-aminolevulinic acid (5-ALA) or 15 mg/mL of ergosterol and 0.5% Tween-80 (YPDE or SCE, respectively) (2).

b. *E. coli* strains, Media, and Growth Conditions. For routine cloning, sub-cloning grade chemically competent *E. coli* cells, strain 10G E. cloni (Lucigen), were used

according to the manufacturer's specifications. For recombinant protein over-expression studies, E. cloni EXPRESS BL21(DE3) chemically competent cells (Lucigen) were utilized according the manufacturer's specifications. In order to characterize the heme sensors in *E. coli*, we employed Δ*hemA*::KAN *E. coli* strains in the MG1655 background (3). Unless otherwise stated, all *E. coli* strains were cultured in Lysogeny broth (LB) (4) with the appropriate antibiotic selection, either 100 μg/mL ampicillin or kanamycin. Transformation of Δ*hemA* cells with a yeast/E. coli shuttle plasmid encoding HS1-M7A, p415-TEF-HS1-M7A, was accomplished by electroporation (5).

c. Human Embryonic Kidney (HEK293) cells, Media, and Growth Conditions. HEK293 cells were plated and transfected in 60 mm X 15 mm polystyrene-coated sterile dishes (Corning) for flow cytometry, and in 35 mm glass bottom dishes (CELLview^{TM}) for microscopy experiments. The cells were plated on day 0 in basal growth medium (Dulbecco's modified eagle medium (DMEM) containing 10% fetal bovine serum and 1% (penicillin-streptomycin). On day 2, cells were transfected with 1 μg of the respective plasmids (pcDNA3.1-HS1 or pcDNA3.1-HS1-M7A) using Lipofectamine 2000 (Invitrogen) in DMEM containing heme-depleted serum (10%) and 0.5mM succinyl acetone, an inhibitor of heme biosynthesis (6). Twenty-four hours after transfection, the media was replaced with fresh DMEM containing heme-depleted serum (10%) and 0.5 mM succinylacetone, and supplemented with 25 or 50 μM of heme. After 16 hours of heme repletion, cells were imaged by confocal microscopy or harvested for flow cytometry, as described in the Experimental Methods. For flow cytometry, cells were rinsed in phosphate buffered saline (PBS), trypsinised, and the cell pellet was washed and resuspended in PBS.

d. Plasmids. *Heme Sensor (HS1) Expression Plasmids.* The synthetic gene for Heme sensor 1, **HS1**, was obtained from GENSCRIPT as codon optimized constructs for expression in yeast/*E. coli* or human cell lines. **HS1** was generated by fusing **mKATE2** (7, 8) and **CG6** (9).

The amino acid sequence of **HS1** is as follows:

HMVSELIKENMHMKLYMEGTVNNHHFKCTSEGEGKPYEGTQTMRIKAVEGGPLPFAFDILAT
SFMYGSKTFINHTQGIPDFFKQSFPEGFTWERVTTYEDGGVLTATQDTSLQDGCLIYNVKIR
GVNFPSNGPVMQKKTLGWEASTETLYPADGGLEGRADMALKLVGGGHLICNLKTTYRSKKPA
KNLKMPGVYYVDRRLERIKEADKETYVEQHEVAVARYCDLPSKLGHRGGSMVSKGEELFTGV
VPILVELDGDVNGHKFSVSGEGEGDATFGGSADLEDNMETLNDNLKVIEKADNAAQVKDALT
KMRAAALDAQKATPPKLEDKSPDSPEMKDFRHGFDILVGQIDDALKLANEGKVKEAQAAAEQ
LKTTRNAYHQKYRGGKLTLKFICTTGKLPVPWPTLVTTLGYGVQCFSRYPDHMKQHDFFKSA
MPEGYVQERTIFFKDDGNYKTRAEVKFEGDTLVNRIELKGIDFKEDGNILGHKLEYNYNSHN
VYIMADKQKNGIKVNFKIRHNIEDGSVQLADHYQQNTPIGDGPVLLPDNHYLSTQSALSKDP
NEKRDHMVLLEFVTAAGITLGMDELYK

Red = mKATE2
Black = Linkers
Green = EGFP
Blue = Cyt b_{562}

Bold = Heme Iron Coordinating Residues

For yeast and *E. coli* expression, **CG6** and **mKATE2** were ordered as two separate gene constructs from GENSCRIPT. The **CG6** gene was flanked by 5'/3' BamHI/HindIII sites and subcloned into plasmid pUC57.

The DNA sequence for E. coli/yeast codon optimized **CG6** is as follows:

```
ATGGTGTCCAAAGGTGAAGAACTGTTTACTGGTGTAGTGCCGATTTTAGTTGAATTAGACGG
TGATGTGAATGGTCATAAGTTTAGCGTGTCGGGTGAAGGCGAAGGTGATGCTACCTTTGGTG
GCTCTGCAGATCTGGAAGACAACATGGAAACTCTGAACGATAACTTGAAGGTTATCGAAAAG
GCCGATAATGCTGCACAAGTGAAAGACGCGTTAACAAAGATGCGCGCCGCGGCTTTGGATGC
TCAGAAAGCAACGCCACCGAAACTGGAGGATAAGTCTCCTGACTCACCAGAAATGAAAGATT
TTCGTCATGGCTTCGACATTTTAGTGGGTCAAATCGATGACGCCTTGAAACTGGCGAACGAG
GGTAAAGTCAAGGAAGCTCAAGCAGCCGCGGAACAGCTGAAGACCACTCGTAATGCATATCA
TCAGAAATACAGAGGTGGCAAACTGACCTTGAAGTTTATCTGTACAACGGGTAAACTGCCTG
TTCCATGGCCGACTTTGGTGACCACTCTGGGCTATGGTGTACAATGCTTCTCACGTTACCCA
GATCATATGAAACAGCACGACTTTTTCAAGAGCGCCATGCCGGAAGGCTACGTTCAAGAACG
CACTATTTTCTTTAAGGATGACGGTAACTACAAGACACGTGCGGAAGTCAAATTTGAAGGCG
ATACGCTGGTAAACAGAATCGAATTGAAGGGTATCGATTTCAAGGAAGACGGCAACATCTTG
GGTCATAAATTGGAATACAACTACAACTCCCACAACGTCTACATCATGGCTGATAAGCAAAA
GAATGGCATCAAGGTAAACTTCAAGATCAGACATAACATCGAAGATGGTTCTGTTCAGCTGG
CTGACCACTATCAACAGAATACACCTATTGGCGATGGTCCGGTGCTGTTACCTGATAACCAT
TACTTGAGCACGCAGAGTGCACTGTCCAAAGATCCAAATGAAAAGCGCGACCACATGGTCTT
GTTGGAATTTGTCACCGCTGCTGGTATCACTTTGGGTATGGATGAACTGTATAAATGA
```

The **mKATE2** gene did not include a stop codon and was flanked by 5'/3' XbaI/BamHI sites and subcloned into plasmid pUC57.

The DNA sequence for E. coli/yeast codon optimized **mKATE2** is as follows:

```
CATATGCACATGGTATCGGAACTGATCAAGGAAAACATGCACATGAAGCTGTATATGGAAGG
CACGGTCAACAACCACCACTTTAAATGCACCTCAGAAGGCGAAGGTAAACCTTATGAAGGTA
CCCAAACTATGAGAATTAAGGCTGTCGAAGGTGGCCCACTGCCGTTTGCCTTCGATATCTTA
GCGACTTCTTTTATGTACGGCTCAAAGACATTCATCAACCATACGCAAGGTATCCCAGATTT
CTTTAAACAGTCCTTTCCGGAAGGCTTCACCTGGGAACGCGTTACCACTTATGAAGACGGTG
GCGTGCTGACAGCTACGCAAGATACTTCGTTACAGGACGGTTGTTTGATTTACAACGTCAAA
ATCCGTGGCGTAAATTTTCCTAGCAACGGTCCAGTCATGCAGAAAAAGACATTAGGCTGGGA
AGCTAGTACCGAAACTTTGTATCCGGCAGATGGTGGCCTGGAAGGTCGCGCTGACATGGCAC
TGAAATTAGTAGGTGGCGGTCACTTGATTTGCAATCTGAAGACAACGTACCGTAGTAAAAAG
CCGGCCAAAAACTTAAAGATGCCTGGTGTTTATTACGTGGATCGTAGATTGGAAAGAATCAA
AGAAGCGGACAAGGAAACGTATGTGGAACAGCACGAAGTCGCCGTCGCACGCTACTGTGATT
TACCGTCCAAGTTAGGTCATAGAGGT
```

For expression in human cell lines, **HS1** was ordered as a codon-optimized single fusion gene construct from GENSCRIPT.

ATGCACATGGTCAGCGAGCTGATCAAGGAAAACATGCACATGAAACTGTACATGGAGGGGAC
TGTGAACAATCACCATTTCAAATGCACCTCCGAGGGCGAAGGGAAGCCCTACGAGGGCACAC
AGACTATGAGGATCAAGGCAGTGGAGGGAGGACCACTGCCATTCGCCTTTGACATTCTGGCT
ACCTCATTCATGTACGGCAGCAAAACCTTCATCAATCACACTCAGGGGATTCCCGACTTCTT
TAAGCAGTCTTTCCCTGAAGGCTTTACTTGGGAGCGAGTGACCACATACGAGGATGGAGGCG
TCCTGACCGCCACACAGGACACAAGTCTGCAGGATGGCTGTCTGATCTATAACGTGAAGATT
CGCGGGGTCAACTTTCCCAGTAATGGACCTGTGATGCAGAAGAAAACCCTGGGATGGGAGGC
TTCAACTGAAACCCTGTACCCAGCAGACGGAGGACTGGAGGGACGAGCAGATATGGCTCTGA
AACTGGTGGGCGGGGGACACCTGATCTGCAACCTGAAGACTACCTATCGGTCCAAGAAACCT
GCTAAGAATCTGAAAATGCCAGGCGTGTACTATGTGGACCGGAGACTGGAGAGAATTAAGGA
AGCAGATAAAGAGACCTACGTGGAGCAGCACGAAGTGGCTGTCGCACGATATTGTGACCTGC
CTTCTAAACTGGGCCATCGGGGCGGGTCTATGGTGAGTAAGGGCGAGGAACTGTTCACAGGG
GTGGTCCCAATCCTGGTGGAACTGGACGGCGATGTCAATGGGCACAAGTTCAGCGTGTCCGG
AGAGGGAGAAGGGGACGCAACCTTTGGAGGCAGCGCCGACCTGGAAGATAATATGGAGACAC
TGAACGATAATCTGAAAGTGATCGAGAAAGCCGACAACGCCGCTCAGGTCAAGGATGCTCTG
ACTAAAATGAGGGCAGCCGCTCTGGATGCACAGAAAGCCACCCCCCCTAAGCTGGAAGACAA
ATCACCTGATAGCCCAGAGATGAAGGACTTCCGCCACGGATTTGATATCCTGGTCGGCCAGA
TTGACGATGCTCTGAAGCTGGCAAATGAAGGCAAGGTGAAAGAGGCACAGGCAGCCGCTGAG
CAGCTGAAAACAACTAGGAACGCCTACCATCAGAAGTATCGCGGGGGAAAGCTGACACTGAA
ATTCATCTGCACCACAGGCAAGCTGCCCGTGCCCTGGCCAACTCTGGTCACTACCCTGGGAT
ACGGCGTGCAGTGTTTTTCCCGCTATCCAGACCACATGAAGCAGCATGATTTCTTTAAATCT
GCCATGCCCGAAGGCTACGTGCAGGAGAGAACCATCTTCTTTAAGGACGATGGAAACTATAA
AACAAGGGCTGAAGTGAAGTTCGAGGGAGACACTCTGGTCAACCGCATCGAACTGAAGGGCA
TTGACTTTAAAGAGGATGGAAATATTCTGGGCCACAAGCTGGAATACAACTATAATAGCCAT
AACGTGTACATCATGGCCGATAAGCAGAAAAACGGCATTAAGGTCAATTTCAAAATCCGGCA
CAATATTGAGGACGGGAGCGTGCAGCTGGCCGATCATTACCAGCAGAACACCCCAATCGGGG
ACGGACCAGTGCTGCTGCCCGATAATCACTATCTGTCCACACAGTCTGCCCTGAGTAAGGAC
CCTAACGAAAAAAGAGATCACATGGTGCTGCTGGAGTTTGTCACCGCAGCCGGGATTACACT
GGGAATGGACGAGCTGTACAAGTGA

For yeast expression, **HS1** was generated by sub-cloning the 5' XbaI/3' BamHI **mKATE2** fragment and the 5' BamHI/3' HindIII **CG6** fragment into p415-ADH1, p415-TEF, and p415-GPD yeast centromeric plasmids (10). The BamHI site between the mKATE2 and CG6 gene sequences create a Gly Ser linker between the mKATE2 and CG6 domains.

For *E. coli* expression, **HS1** was sub-cloned into a variant of pET30a(+) (EMD Millipore), pAR1008. pAR1008 is derived from pET30(+), but has a Tobacco Etch Virus (TEV) protease site (ENLFYQS) flanked by a 3' BamHI site in place of the original thrombin protease site. Sub-cloning of a 5'/3' BamHI/BamHI fragment of **mKATE2** and a 5'/3' BamHI/HindIII **CG6** fragment, both generated by PCR, results in an expression plasmid that has a His_6 tag, followed by a TEV protease site linked to HS1 via a Gly Ser linker.

For expression in human cell lines, the human codon optimized **HS1** gene was sub-cloned into the 5' BamHI and 3' XhoI site of pcDNA3-EGFP (Addgene). This plasmid drives protein expression using a CMV promoter.

Heme Sensor Variants. PCR based mutagenesis was used to generate variants of HS1 with an additional Gly Ser linker between mKATE2 and CG6, or with mKATE2 at the C-terminus of CG6. For the latter, one or two (Gly Ser) linkers between CG6 and mKATE2 were introduced. In addition, a stop codon was introduced into mKATE2 using Quick Change mutagenesis (Agilent Technologies). These constructs are highlighted in **Figure S7** and are driven by the GPD promoter in p415-GPD. Using similar PCR based approaches, an mKATE2-EGFP fusion construct lacking Cytochrome b_{562} was generated and sub-cloned into appropriate expression yeast, *E. coli*, or mammalian cell expression plasmids.

For mitochondrial matrix or nuclear targeting in yeast, heme sensors were fused to N-terminal Cox4 (11) or C-terminal SV40 (12) localization sequences, respectively. For mitochondrial matrix targeting, a Cox4 matrix-targeting pre-sequence was amplified from yeast genomic DNA with a 5' SpeI site and a 3' HindIII site. HS1 was PCR amplified to include a 5' HindIII site and a 3' SalI site. The Cox4 and HS1 amplicons were then sub-cloned into the SpeI and SalI sites of p415-TEF.

For nuclear targeting, HS1 was PCR amplified using mutagenic primers that incorporate the SV40 NLS sequence (5'-CCTAAGAAGAAGAGGAAGGTT-3') prior to the stop codon. The HS1-SV40 amplicon included 5' SpeI and and 3' HindIII sites for sub-cloning into p415-GPD.

For all expression plasmids, heme binding site mutations of HS1 in which Met_7 or His_{102} are mutated to Ala were generated by Quick Change mutagenesis (Agilent Technologies). The numbering refers to its position in Cytochrome b_{562}, and is highlighted in bold in the sequence for HS1.

hem1::HIS3 Knockout Plasmid and hem1Δ Strain Generation. In order to generate a *hem1*::HIS3 knockout plasmid, the 5' and 3' untranslated regions (UTR's) of *HEM1* were amplified from yeast genomic DNA. The 5' UTR (-300 to +7) was amplified to include 5' BamHI and 3' SalI sites. The 3' UTR (+1695 to +2195) was amplified to include 5' EagI and 3' BamHI sites. The 5' and 3' UTRs were digested with the enzymes indicated and ligated in a trimolecular reaction into the *HIS3* integrating plasmid pRS403 (13) digested with EagI and SalI, resulting in pDH001. Transformation of BY4741 with pDH001 linearized with BamHI resulted in deletion of *HEM1* sequences from +8 to +1694. *hem1Δ* cells were initially selected for on SC-HIS media supplemented with 50 µg/mL 5-ALA. After isolation of single colonies, *bona fide hem1Δ* cells were selected for their heme auxotrophy. That is to say, strains that exhibited limited growth in YPD or SC media, and robust growth in media supplemented with 50 µg/mL of 5-ALA or hemin, were deemed genuine *hem1Δ* cells.

HAP1 Transcriptional Reporter, pr^{CYC1}-EGFP. In order to monitor HAP1 activity, a transcriptional reporter was generated in which EGFP was driven by the CYC1 promoter, which is a gene that is positively regulated by HAP1. A 5'/3' BamHI/HindIII EGFP fragment was amplified and sub-cloned in p416-CYC1, containing the CYC1 promoter.

2. Protein Purification

pET30a(+) plasmids containing genes for HS1 and related variants were expressed in *E. coli* BLD21(DE3) cells. Cells were pre-cultured overnight for 14-16 hours in 25 mL of LB media with 50 µg/mL kanamycin at 37° C. This 25 mL culture was then used to inoculate 1 L of fresh LB media supplemented with 50 µg/mL kanamycin. The resulting cultures were grown at 20 °C to an OD_{600} = 0.8 when protein expression was induced with the addition of 100 mM isopropyl β-D-thiogalactopyranoside (IPTG). Cultures were incubated at 20 °C for an additional 48 h. Cells were harvested and resuspended in 30 mL of lysis buffer (20 mM Tris, 100 mM NaCl, pH 8.0, 1 mM PMSF, 1X ProteaseArrest™, 10 µg/mL DNaseI). Cells were disturbed using a French Pressure Cell (two passes on high at 1200 psi, 4 °C). The lysate was clarified by centrifugation (20000 rpm, 4 °C, 30 min). Total protein concentration was determined by the Bradford method, using bovine serum albumin as a standard (14). Heme sensor proteins from the cell-free extract were purified on an AKTA Prime plus FPLC (GE Healthcare). Cell-free protein extracts were loaded onto a 20 mL HisPrep FF 16/10 column pre-packed with Ni sepharose (GE Healthcare) after being equilibrated with 10 column volumes of low imidazole buffer A (20 mM Tris, 100 mM NaCl, pH 8.0, 20 mM imidazole). After washing the protein extract on the column with buffer A, heme sensor proteins were eluted by gradient elution, going from 100% buffer A to 100% buffer B (300 mM imidazole, 20 mM Tris, 100 mM NaCl, pH 8.0 buffer), over 15 column volumes (300 mL). 10 mL fractions were collected and purity was monitored by SDS-PAGE. Fractions containing the heme sensor proteins were pooled and dialyzed against TEV cleavage buffer (20 mM Tris, 100 mM NaCl, pH 8.0). The following day, the His_6-tag was cleaved by adding 1 molar equivalent of TEV protease for 18 hours at room temperature. TEV protease was pre-prepared precisely as described previously (15). Following cleavage by TEV protease, the protein was loaded onto a 1 mL HisTrap HP column prepacked with Ni sepharose (GE Healthcare) and eluted using low imidazole buffer A in 1 mL fractions. After elution, purity was checked via SDS-PAGE. The fractions containing heme sensor were again pooled and loaded onto a HiTrap Q HP 1 mL cation exchange column (GE Healthcare) after equilibrating with 10 column volumes of low ionic strength buffer A (20 mM Tris, 10 mM NaCl, pH 8.0). The protein on the column was washed with 5 column volumes of buffer A at 1 mL/min and then equilibrated with 10% high ionic strength buffer B (20 mM Tris, 1 M NaCl, pH 8.0). The protein was then eluted with a gradient of 10 to 25% buffer B over 30 column volumes, or 30 mL, at a flow rate of 1 mL/min, collecting 300 µL fractions. Once purity was confirmed via SDS-PAGE analysis, fractions were stored at 4 °C, and used for all analyses within 2 weeks of purification. Typical purifications gave yields of ~3 mg of heme sensor per 1 L of culture. Prior to use for experiments, pure fractions were buffer exchanged into appropriate pH buffered solutions using 10 kDa cut-off protein concentrators (Pierce, Thermo Fisher Scientific).

Representative purities of fractions are depicted in **Figs. S2B** and **S2F**.

3. Experimental Methods

a. Instrumentation. All UV/visible absorbance spectra were recorded on a Cary 60 spectrophotometer. Fluorescence measurements were collected on a Cary Eclipse fluorescence spectrophotometer or a Synergy Mx multi-modal plate reader. Flow cytometry was performed on a BD FACS Aria III Cell Sorter or BD LSR II Flow Cytometer, with data analysis accomplished using FlowJo v9.9.3 software. Confocal laser scanning microscopy was accomplished using a Zeiss ELYRA LSM 780 Super-resolution Microscope, with all images processed in ImageJ (16). Quantifications of metal and heme stock solutions were accomplished by total reflection x-ray fluorescence (TXRF) on a Bruker S2 Picofox TXRF. Measurement for cellular heme was accomplished by high-pressure liquid chromatography (HPLC) on an Agilent 1260 Infinity HPLC with a diode array detector. All protein purifications were accomplished on an AKTA Prime plus FPLC (GE Healthcare).

b. *In vitro* Characterization of Heme Sensors. Heme sensor protein, HS1, and related variants, were re-constituted into 20 mM $Na_2HPO_4^{2-}$, 100 mM NaCl, pH = 8.0 buffer and quantified by measuring sulfur content using total reflection X-ray fluorescence (TXRF) and by the Bradford assay. Both measurements gave molar concentrations of sensor within 3% of each other. UV/visible spectrophotometry of dilutions of HS1 and related variants revealed extinction coefficients at 488 nm (EGFP) and 588 nm (mKATE2) of $\varepsilon_{488\ nm}$ = 52631 cm^{-1} M^{-1} and $\varepsilon_{588\ nm}$ = 43859 cm^{-1} M^{-1}. These extinction coefficients were used for routine protein quantifications for all analyses.

5-10 mM hemin chloride stock solutions were made in 0.1 M NaOH and filtered through a 0.2 µm syringe filter (Amicon). Stock solutions were quantified by measuring iron content using TXRF. UV/visible spectrophotometry of dilutions of heme stock solutions gives a hemin extinction coefficient at 612 nm of $\varepsilon_{612\ nm}$ = 4431 cm^{-1} M^{-1} or $\varepsilon_{385\ nm}$ = 58,400 $M^{-1}cm^{-1}$. Appropriate working dilutions of hemin chloride were made in .1 M NaOH such that titration involved delivery of ~.1 equivalents of heme relative to protein in 0.2-0.4 µL volumes using a hand-held gas tight Hamilton syringe. In order to ensure heme had not aggregated/precipitated, we titrated hemin into solutions of well-defined single site hemoproteins like *apo*-myoglobin or *apo*-Cytochrome b_{562}. We consistently observed a 1:1 heme to protein stoichiometry. If heme were precipitating/aggregating between pH 6.0 and 9.0, we would expect deviations in the equivalency point required to saturate these hemoproteins. These protein solutions were standardized by measuring sulfur content via total reflection X-ray fluorescence spectroscopy (TXRF).

Ferric heme titrations were accomplished by titrating 0.1-0.2 equivalents of hemin chloride into buffered aqueous solutions of HS1 and related variants over a broad pH range. All buffers included 100 mM NaCl. For titrations between pH values of 5.0 and 5.5, a mixed phosphate-citrate buffer was used (17). For pH values between 5.5 and 6.5, 20 mM MES was utilized. For pH values between 6.5 and 7.0, 20 mM PIPES was utilized. For pH values between 7.0 and 8.0, 20 mM HEPES was utilized.

For pH values between 8.0 and 9.0, a 20 mM sodium phosphate buffer was utilized. We also employed 20 mM NaP_i for pH values between 6 and 9 and 20 mM sodium acetate for pH values between 4.5 and 6. The composition of the buffer (not including the pH) did not impact the observed fluorescence or absorbance values or thermodynamic data. All buffers were adjusted to the appropriate pH using 6 M HCl or NaOH. Prior to titrations, all buffers were degassed and were performed in 1 cm path length quartz cuvettes that were maintained anaerobically with rubber septa.

Ferrous heme titrations were accomplished similarly to ferric heme titrations, but with 1 mM ascorbate present as a reductant (9). Sodium dithionite, which is typically used to reduce heme, could not be used due to its ability to reduced and quench EGFP and mKATE2 fluorescence. All buffers were de-gassed and samples were manipulated in a COY anaerobic chamber maintained in an atmosphere of 5% H_2 and 95% N_2.

Titrations were accomplished using sensor concentrations spanning 10 nM to 500 nM. Heme titrations were monitored by fluorimetry on a Cary Eclipse fluorimeter and, if protein concentrations were ~500 nM, by absorbance spectroscopy using a Cary 60 spectrophotometer.

Heme sensor fluorescence ratios were monitored by recording the ratio of EGFP (ex. 488, em. 510 nm) and mKATE2 (ex. 588 nm, em. 620 nm) fluorescence values.

Ferric and ferrous heme binding affinities were derived using a 1:1 heme:protein binding model as done previously (18-24). Specifically, titration data were fit with the equilibrium model depicted in equations S1 and S2 using non-linear least squares regression analysis software KaleidaGraph 4.5 (Synergy Software).

$$\mathrm{ML} = .5 \times \left(K_{\mathrm{D1}} + \mathrm{L_T} + \mathrm{M_T} - \sqrt{\left(-K_{\mathrm{D1}} - \mathrm{L_T} - \mathrm{M_T}\right)^2 - 4\mathrm{L_T}\mathrm{M_T}} \right) \quad \text{Equation S1}$$

$$F = F_L + \Delta F * [ML] \quad \text{Equation S2}$$

Where K_{D1} is the ferric or ferrous (in presence of ascorbate) heme dissociation constant, L_T is the concentration of protein, ML is the concentration of the heme-protein complex, M_T is the concentration of heme that is being titrated, F is the fluorescence signal at any given concentration of heme, F_L is the initial fluorescence of the protein in the absence of heme, and ΔF is the change in fluorescence due to heme binding.

For data fitting, F_L, ΔF, L_T, and M_T were treated as fixed parameters derived from experiments, and the K_D was a “floating” parameter that was derived from regression analysis. The fluorescence signals utilized to determine K_D were either the emission at 510 nm upon excitation at 488 nm (EGFP) or the ratio of the fluorescence signals derived from emission at 510 nm upon excitation at 488 nm (EGFP) and emission at 620 nm upon excitation at 588 nm (mKATE2), otherwise referred to as the

EGFP:mKATE2 fluorescence ratio. The K_D's derived from the heme dependence of EGFP fluorescence or the EGFP:mKATE2 fluorescence ratio were typically within a factor of 2 of each other and within the limits of the standard deviation associated with replicate titrations.

For pH titrations, *apo* or *holo* sensors were diluted to a concentration of 100 nM in various pH buffered solutions. For pH titrations, *holo* sensor was incubated with 1 equivalent of heme, along with 1 mM ascorbate to maintain reducing conditions.

For measurements of heme selectivity, *apo* or *holo* sensors were incubated with the indicated concentrations of metal salts, protoporphyrin IX (PPIX), biliverdin (BV), or bilirubin (BR). The concentrations of metal stock solutions were determined by TXRF.

c. Characterization of Heme Sensors in Yeast. For all sensor fluorescence measurements, WT and *hem1*Δ yeast cells expressing the heme sensors were cultured in SCE-LEU media for ~14-16 hours to mid-exponential phase (an optical density at 600 nm of $OD_{600\ nm}$ ~ 1-2. Unless otherwise noted, all cytosolic measurements were accomplished with the indicated sensor proteins expressed on the p415-GPD plasmid, a low copy centromeric (CEN) plasmid with a GPD promoter (10). Nuclear and mitochondrial matrix targeted sensors were expressed on p415-GPD and p415-TEF plasmids, which are low copy centromeric (CEN) plasmids with GPD and TEF promoters, respectively (10). After culturing, cells were harvested, washed in water, and resuspended in phosphate buffered saline (PBS) solution at concentrations between 3 and 5 $OD_{600\ nm}$/mL, or 6 x 10^7 to 1 x 10^8 cells/mL. For fluorimetry measurements on a population of cells, fluorescence was recorded on a Synergy Mx multi-modal plate reader using black Greiner Bio-one flat bottom fluorescence plates. EGFP and mKATE fluorescence were recorded using excitation and emission wavelength pairs of 488 nm and 510 nm and 588 nm and 620 nm, respectively. Background fluorescence of cells not expressing the heme sensors were recorded and subtracted from the EGFP and mKATE2 fluorescence values.

The impact of nitric oxide (NO), superoxide (O_2^-), hydrogen peroxide (H_2O_2), and glutathione oxidation on intracellular heme dynamics was determined by incubating 6 x 10^7 to 1 x 10^8 cells/mL of cells expressing the heme sensor in PBS with the indicated concentrations of NOC-7 (Enzo Life Sciences), paraquat, H_2O_2, and diamide, respectively. The kinetics of heme mobilization were monitored by measuring the EGFP to mKATE2 ratios as described above.

For quantitative heme monitoring, we developed an *in-situ* method to calibrate the sensor in cells similar to that previously described (25). The concentration of [heme] accessible to the sensor is governed by the following expression (26):

$$[\mathrm{heme}] = K_D \times \frac{R_{expt} - R_{min}}{R_{max} - R_{expt}} \left(\frac{F_{min}^{mKATE2}}{F_{max}^{mKATE2}} \right) \qquad \text{Equation S3}$$

K_D is the heme-heme sensor dissociation constant, R_{expt} is the EGFP:mKATE2 fluorescence ratio under any given condition, R_{min} is the EGFP:mKATE2

fluorescence ratio when 0% of the sensor is bound to heme, R_{max} is the EGFP:mKATE2 fluorescence ratio when 100% of the sensor is bound to heme, F_{min}^{mKATE2} is the mKATE2 emission intensity when 0% of the sensor is bound to heme, and F_{max}^{mKATE2} is the mKATE2 emission intensity when 100% of the sensor is bound to heme.

Determination of R_{max} and F_{max}^{mKATE2} involves recording EGFP and mKATE2 fluorescence after digitonin permeabilization of cells and incubation with 50 µM heme. Briefly, 3 to 5 $OD_{600\ nm}$/mL of cells are resuspended in PBS with 100 µg/mL of digitonin, 1 mM ascorbate, and 50 µM hemin chloride. After a 30 minute incubation at 30°C, cells were harvested, washed, and resuspended in PBS buffer prior to recording of fluorescence by plate reader, flow cytometry, or microscopy.

Determination of R_{min} and F_{min}^{mKATE2} involves recording EGFP and mKATE2 fluorescence after cells are treated with the heme biosynthesis inhibitor succinylacetone (27) or from *hem1*Δ cells cultured in parallel.

Since digitonin cannot permeabilize mitochondrial or nuclear membranes, we devised an alternative strategy to determine R_{max} and F_{max}^{mKATE2}. This procedure involved digesting the yeast cell wall with Zymolyase, followed by incubating yeast spheroplasts with .1% Triton-X100, to permeabilize all membranes, as well as 1 mM ascorbate and 50 µM hemin chloride. Briefly, cells were grown to a density of 1-2 $OD_{600\ nm}$/mL, washed in sterile Milli-Q water, and resuspended in “softening buffer” (100 mM Tris-HCl, pH = 9.4, 10 mM DTT) at a concentration of 10 $OD_{600\ nm}$/mL of cells. Cells were incubated at room temperature, with occasional swirling, for 30-60 minutes. Cells were then washed and resuspended in a sorbitol buffer containing 50 mM Tris-HCl, pH 7.4, 1.2 M Sorbitol. To this cell suspension in sorbitol buffer, .5 mg/mL of 100-T Zymolyase (MP Biomedicals, VWR) was added, followed by incubated for 45 minutes at 30 °C with occasional inversion. Next, cells were washed and resuspended in sorbitol buffer (50 mM Tris-HCl, pH 7.4, 1.2 M Sorbitol). 3 to 5 $OD_{600\ nm}$/mL of cells in Sorbitol buffer were resuspended in a sorbitol buffer that contained .1% Triton X-100, 2 mM Ascorbate, and 50 µM hemin chloride, and incubated at 30 °C for 30-45 minutes. Cells were then washed and resuspended in sorbitol buffer for fluorescence measurments.

Flow cytometric measurements were performed using a BD FACS Aria lll Cell Sorter or BD LSR II Flow Cytometer, both equipped with an argon laser (ex 488nm) and yellow-green laser (ex 561nm). EGFP was excited using the argon laser and was measured using a 530/30nm bandpass filter. mKATE2 was excited using the yellow-green laser and was measured using a 610/20nm bandpass filter. Data evaluation was conducted using FlowJo v9.9.3 software. The number of cells measured per experiment was set to 1,000,000 unless otherwise stated. BY4741 empty vector cells were used as a negative control for fluorescence. Only mKATE2 positive cells were selected for analysis.

Confocal microscopy was done on a Zeiss ELYRA LSM 780 Super-resolution Microscope equipped with a 63x, 1.4 numerical aperture oil objective. EGFP was excited with the 488 nm line of an argon ion laser, while mKATE2 was excited using the 594 nm of a HeNe laser line. The 494-571nm and 606-686 nm band pass filters were used to filter emission for EGFP and mKATE, respectively. Images were collected using Zeiss software and analyzed with ImageJ 1.48v (Rasband, W.S., ImageJ, U. S. National Institutes of Health, Bethesda, Maryland, USA, http://rsb.info.nih.gov/ij/, 1997-2007). Ratio images were generated using ImageJ RatioPlus software (http://rsb.info.nih.gov/ij/plugins/ratio-plus.html) after background subtraction. To confirm mitochondrial or nuclear localization of the sensors, prior to microscopy, exponential phase cells were incubated with 2.5 µg/mL 4', 6-diamidino-2-phenylindole (DAPI) (Invitrogen) in SCE-LEU media for 30 minutes to stain nuclear and mitochondrial DNA.

c. Characterization of Heme Sensors in Human Embryonic Kidney (HEK293) cells. HEK293 cells were plated and transfected in 60 mm X 15 mm polystyrene-coated sterile dishes (Corning) for flow cytometry and in 35 mm glass bottom dishes (CELLview^{TM}) for microscopy experiments. The cells were plated on day 0 in basal growth medium (Dulbecco's modified eagle medium (DMEM) containing 10% fetal bovine serum and 1% (penicillin-streptomycin). On day 2, cells were transfected with 1 µg of heme sensor plasmids pcDNA3.1-HS1 or pcDNA3.1-HS1-M7A using Lipofectamine 2000 (Invitrogen) in DMEM containing heme-depleted serum (10%) and 0.5 mM succinylacetone, an inhibitor of heme biosynthesis (6). Twenty-four hours after transfection, the media was replaced with fresh DMEM containing heme-depleted serum (10%) and 0.5 mM succinyl acetone, and supplemented with 0, 25 or 50 µM heme. After 16 hours of heme repletion, cells were imaged by confocal microscopy similarly to the procedure described for yeast or harvested for flow cytometry. With respect to the latter, HEK293 cells were rinsed in PBS, trypsinised, and the cell pellet was washed and resuspended in PBS for flow cytometry analysis similarly to that described for yeast. 100,000 mKATE positive cells were analyzed.

d. Characterization of Heme Sensors in E. coli cells. *E. coli* strain MG1655 DE3 Δ*hemA* expressing HS1-M7A on the yeast/E coli shuttle plasmid p415-GPD was grown to early exponential phase in Lennox broth with 50 µg/mL 5-ALA. Cells were collected by centrifugation and resuspended in the same volume of LB without 5-ALA. An initial sample was collected at this time (time = 0 min) and additional samples were collected at various time points up to 90 min. After washing and resuspending in 1X PBS, 100 µL of 10 OD/ml cells was used for fluorescence measurements. The EGFP:mKATE2 fluorescence ratios were measured using a Synergy H1 hybrid multi-mode microplate reader (BioTek). A control strain containing pET21a was grown under similar conditions and used for background corrections.

e. Respiration Measurements in Yeast. WT yeast cells expressing empty vector (p415-GPD) or p415-GPD-HS1-M7A were cultured in SC-LEU media for ~14-16 hours to mid-exponential phase (an optical density at 600 nm of $OD_{600\ nm}$ ~ 1-2). Cells were harvested and resuspended in fresh SC-LEU media at a concentration of

1 x 10^8 cells/mL and oxygen consumption was measured using the BD Oxygen Biosensor System precisely as we have done previously (28).

f. Catalase Activity Measurements in Yeast. WT yeast cells expressing empty vector (p415-GPD), or HS1-M7A driven by the GPD, TEF1, or ADH1 promoters (p415-GPD-HS1-M7A, p415-TEF1-HS1-M7A, p415-ADH1-HS1-M7A) were cultured in SC-LEU media for ~14-16 hours to mid-exponential phase (an optical density at 600 nm of $OD_{600\ nm}$ ~ 1-2). Cells were harvested and lysed in phosphate buffer and 10 µg of protein lysate were subjected to native PAGE on a 10% tris-glycine gel (Invitrogen). After electrophoresis, an in-gel activity stain was utilized to measure catalase activity (29). Briefly, a catalase staining solution containing 1 part Dopamine (20mg/mL) in pH 8 0.2 M KP_i buffer, 1 part para-phenylenediamine (3.5mg/mL) in pH 8 0.2M KP_i, 1 part 15 % H_2O_2, and 2 parts DMSO were mixed in the order listed. The staining solution was added directly to the gel and allowed to stain for 2 minutes, followed by rinsing in Milli-Q water and imaging.

g. Heme Quantification in Yeast. Heme was quantified using a protocol adapted from the method of Woods and Simmonds (30). Briefly, yeast were cultured in 25 mL of YPDE media for 15 hours to a density of 1 $OD_{600\ nm}$ /mL. Cells were harvested, washed in ice-cold Milli-Q water, and lysed in three pellet volumes of acid-acetone (9.75 mL acetone, 0.250 mL concentrated HCl). Lysis was achieved at 4 C using one pellet volume of zirconium oxide beads and a bead beater (Bullet Blender, Next Advance) on a setting of 8 for 3 minutes. After homogenization, lysates were clarified by centrifugation at maximum speed on a table-top centrifuge. 50 µL of an acid-acetone extract of heme was diluted into 50 µL of 0.1% trifluoroacetic acid in a 1:1 mixture of water and acetonitrile. Heme was quantitated by HPLC using a flow rate of 1 mL/min and elution gradients going from 50% acetonitrile in water, 0.1% TFA to 100% acetonitrile, 0.1% TFA over 10 minutes on a C-18 column (Poroshell 120, SB-C18, 4.6 x 100 mm, 2.7 um). Heme was quantified relative to hemin chloride standards run in parallel and normalized for cell number. Cellular heme concentration was determined by assuming a yeast cell volume of 50 fL. Heme was unambiguously identified from its retention time and characteristic UV/visible spectrum using a photodiode array detector coupled to the HPLC.

h. HAP1 Transcriptional Reporter Assay. Yeast cells expressing p416-CYC1-EGFP, or EGFP driven by the Hap1p regulated CYC1 promoter, were cultured in 10 mL of SCE-URA media for 15 hours to a to a density of 1 $OD_{600\ nm}$ /mL. Cells were resuspended in PBS to a concentration of 1 x 10^8 cells/mL and 100 uL was used to measure EGFP fluorescence (ex. 488 nm, em. 510 nm). As a positive and negative control, WT and *hem1*Δ cells were cultured for each experiment. Background auto-fluorescence of cells not expressing EGFP was recorded and subtracted from the EGFP expressing strains.

i. Immunoblotting. Yeast were cultured in 10 mL of SC media for 15 hours to a density of 1 $OD_{600\ nm}$ /mL. Cells were harvested, washed in ice-cold Milli-Q water, and lysed in two pellet volumes of phosphate buffer supplemented with protease

inhibitors as described previously (28, 31). Lysis was achieved at 4 C using one pellet volume of zirconium oxide beads and a bead beater (Bullet Blender, Next Advance) on a setting of 8 for 3 minutes (28, 31). Lysate protein concentrations were determined by the Bradford method (Bio-rad) and 12% tris-glycine gels (Invitrogen) were employed for SDS-PAGE (28, 31). Anti-GFP rabbit or anti-GAPDH polyclonal antibodies (Genetex) and a goat anti-rabbit secondary antibody conjugated to a 680 nm emitting fluorophore (Biotium) were used to probe for HS1 and related variants or GAPDH, respectively. All gels were imaged on a LiCOR Odyssey Infrared imager (28, 31).

4. Supporting Figures

Figure S1. Spectral overlap between the normalized EGFP and mKATE2 fluorescence emission and the electronic absorption of ferric and ferrous cytochrome b_{562} (Cyt b_{562}) and hemin chloride. Spectra were collected in 20 mM PIPES, 100 mM NaCl, pH = 7.5. Based on the spectral overlap between EGFP and mKATE2 fluorescence emission and the electronic absorption of Cyt b_{562} , the Forster distances for EGFP-Cyt b_{562} and mKATE2-Cyt b_{562} were calculated to be 46 Å and 20 Å, respectively, as done previously (32).

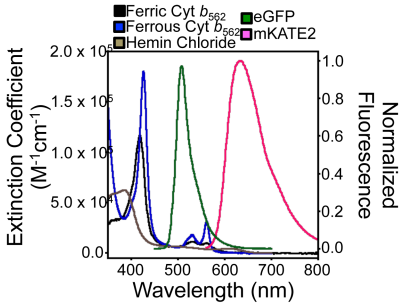

Figure S2. Molecular models, purities, and UV/visible spectra of ferric and ferrous heme bound to HS1 and HS1-M7A. (**A**) Molecular model of the heme sensors HS1 and HS1-M7A. Models are derived from the X-ray structures of mKATE (PDB: 3BXB) and CG6 (PDB: 3U8P). (**B**) Representative purities of HS1 after ion-exchange chromatography on a 12% SDS-PAGE gel and Coomassie staining. (**C**) A ferric heme titration of HS1 and resulting UV/vis spectra. Hemin chloride was titrated into 500 nM HS1 in an aqueous buffered solution (20 mM $Na_2HPO_4^{2-}$, 100 mM NaCl, pH = 8.0). (**D**) A ferrous heme titration of HS1 and resulting UV/vis spectra. Ferrous heme titrations were conducted similarly as in **C**, but with 1 mM ascorbate to maintain reducing conditions. (**E**) Comparison of ferric and ferrous UV/visible spectra at a 1:1 heme:sensor stoichiometry for HS1. (**F**) Representative purities of HS1-M7A after ion-exchange chromatography on a 12% SDS-PAGE gel and Coomassie staining. (**G**) A ferric heme titration of HS1-M7A and resulting UV/vis spectra. Hemin chloride was titrated into 500 nM HS1-M7A in an aqueous buffered solution (20 mM $Na_2HPO_4^{2-}$, 100 mM NaCl, pH = 8.0). (**H**) A ferrous heme titration of HS1-M7A and resulting UV/vis spectra. Ferrous heme titrations were conducted similarly as in **G**, but with 1 mM ascorbate to maintain reducing conditions. (**I**) Comparison of ferric and ferrous UV/visible spectra at a 1:1 heme:sensor stoichiometry for HS1-M7A.

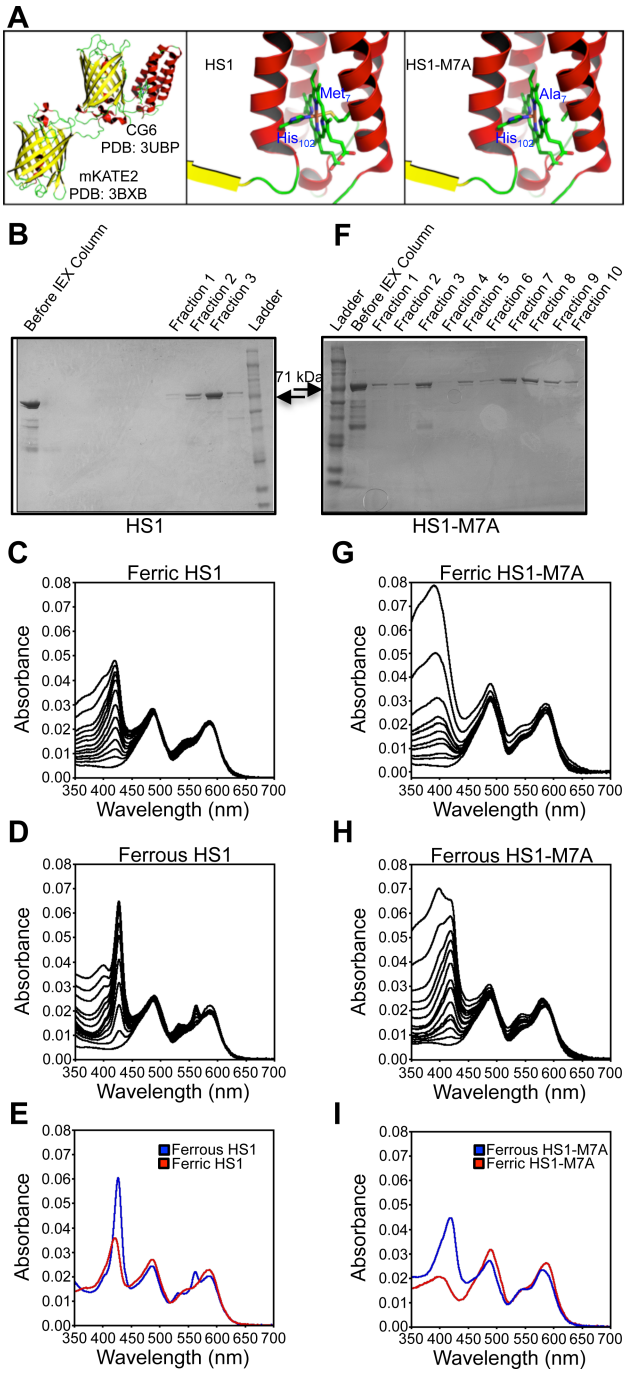
A
CG6
PDB: 3UBP
mKATE2
PDB: 3BXB
HS1
Met7
His102
HS1-M7A
Ala7
His102
B
Before IEX Column
Fraction 1
Fraction 2
Fraction 3
Ladder
71 kDa
HS1
F
Ladder
Before IEX Column
Fraction 1
Fraction 2
Fraction 3
Fraction 4
Fraction 5
Fraction 6
Fraction 7
Fraction 8
Fraction 9
Fraction 10
HS1-M7A
C
Ferric HS1
G
Ferric HS1-M7A
D
Ferrous HS1
H
Ferrous HS1-M7A
E
Ferrous HS1
Ferric HS1
I
Ferrous HS1-M7A
Ferric HS1-M7A
Absorbance
Wavelength (nm)
0.00
0.01
0.02
0.03
0.04
0.05
0.06
0.07
0.08
350 400 450 500 550 600 650 700

Figure S3. Representative ferric and ferrous heme binding isotherms of HS1 and HS1-M7A, their pH-dependence, and the heme binding affinities of other hemoproteins for comparison. (**A**) Titration of hemin chloride into 20 nM HS1. (**B**) Titration of hemin chloride into 10 nM HS1 incubated with 1 mM ascorbate. (**C**) The pH dependence of ferric heme-HS1 K_D^{III} values. (**D**) Titration of hemin chloride into .5 μM HS1-M7A. (**E**) Titration of hemin chloride into 50 nM HS1-M7A incubated with 1 mM ascorbate. (**F**) The pH dependence of ferric and ferrous heme-HS1-M7A K_D^{III} and K_D^{II} values. All representative binding isotherms were conducted in an aqueous buffered solution of 20 mM PIPES, 100 mM NaCl, pH = 7.0. All data were fit to 1:1 heme:sensor binding models. For the pH dependence of the ferric and ferrous HS1 or HS1-M7A heme dissociation constants, the K_D^{III} or K_D^{II} values represent the mean ± SD of triplicate titrations at each pH value. (**G**) Survey of heme binding affinities of hemoproteins typically encountered in biology, including globins and cytochromes (33), hemopexin (34), heme oxygenase 1 (35), heme oxygenase 2 (36), Reverbβ (37), human serum albumin (38), and heme regulatory motifs of various heme-dependent transcription factors (39). All affinities are reported for hemin (ferric Fe(III)-heme). Ferrous heme affinities are largely unreported.

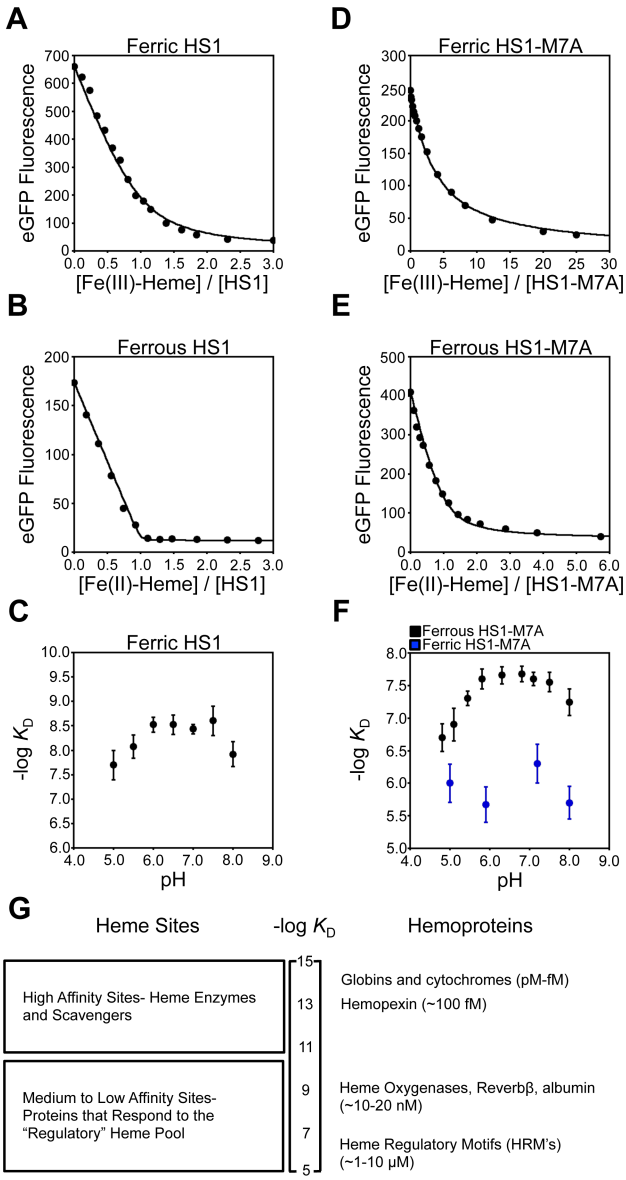
A
Ferric HS1
eGFP Fluorescence
[Fe(III)-Heme] / [HS1]
D
Ferric HS1-M7A
eGFP Fluorescence
[Fe(III)-Heme] / [HS1-M7A]
B
Ferrous HS1
eGFP Fluorescence
[Fe(II)-Heme] / [HS1]
E
Ferrous HS1-M7A
eGFP Fluorescence
[Fe(II)-Heme] / [HS1-M7A]
C
Ferric HS1
-log K_D
pH
F
Ferrous HS1-M7A
Ferric HS1-M7A
-log K_D
pH

G
Heme Sites
-log K_D
Hemoproteins
High Affinity Sites- Heme Enzymes and Scavengers
Medium to Low Affinity Sites- Proteins that Respond to the "Regulatory" Heme Pool
15
13
11
9
7
5
Globins and cytochromes (pM-fM)
Hemopexin (~100 fM)
Heme Oxygenases, Reverbβ, albumin (~10-20 nM)
Heme Regulatory Motifs (HRM's) (~1-10 μM)

Figure S4. Ferrous heme selectivity and pH/concentration-dependent fluorescence of HS1 and HS1-M7A. (**A-B**) Selectivity of (**A**) HS1 or (**B**) HS1-M7A for ferrous heme over other metals, protoporphyrin IX (PPIX), biliverdin (BV), and bilirubin (BR). 50 nM HS1 or HS1-M7A was incubated in an aqueous buffered solution (20 mM PIPES, 100 mM NaCl, 1 mM ascorbate, pH 7.4) with 50 equivalents of the indicated analytes and/or 1 equivalent of ferrous heme. (**C-D**) The pH-dependence of the fluorescence ratios of 100 nM *apo*- and *holo*- (**C**) HS1 or (**D**) HS1-M7A. 500 nM HS1 or HS1-M7A was incubated in 20 mM NaP_i (pH 6-9) or 20 mM sodium acetate (pH 4.5-6), 100 mM NaCl, and 1 mM ascorbate with (*holo*) or without (*apo*) 1 equivalent of heme. (**E**) The concentration dependence of the fluorescence ratios of HS1 and HS1-M7A. For (**A-E**), the EGFP:mKATE2 fluorescence ratios (EGFP, ex. 488, em. 510; and mKATE2, ex. 588, em. 620 nm) were recorded after 16 hours of equilibration in an anaerobic chamber (95% N_2, 5% H_2). All data represent the mean ± SD of triplicates.

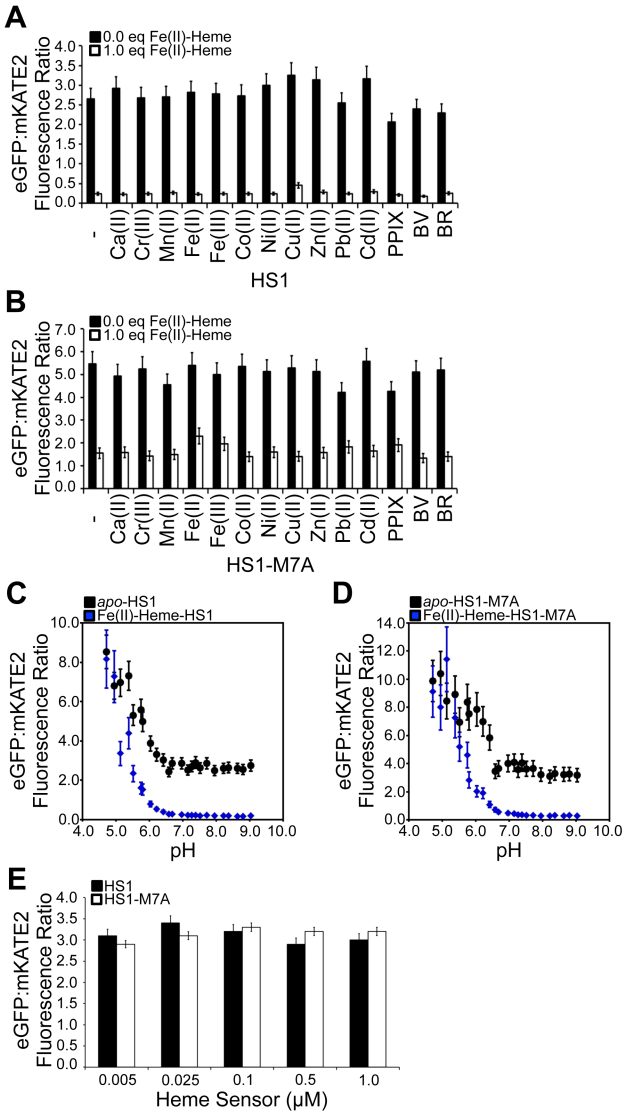

Figure S5. Reversibility of ferrous heme binding to HS1 and HS1-M7A and concentration dependent fluorescence of the sensors. 100 nM (**A**) HS1 or (**B**) HS1-M7A were incubated in an aqueous buffered solution (20 mM PIPES, 100 mM NaCl, 1 mM ascorbate, pH 7.0) and the EGFP:mKATE2 fluorescence ratios were recorded over time as 1.0 equivalent of heme and 100 equivalents of *apo*-Cyt b_{562} was added at -2.5 and 0 minutes, respectively. The kinetic traces are representative of two independent trials.

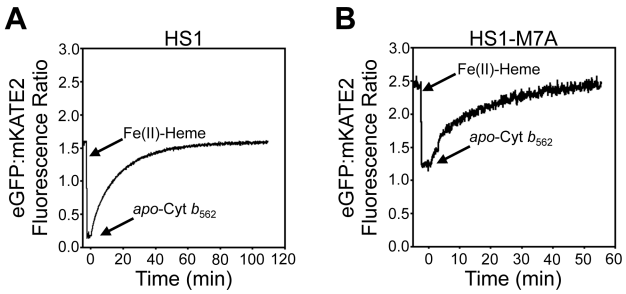

Figure S6. Heme dependence of cellular EGFP:mKATE2 fluorescence ratios. (**A-B**) WT cells expressing (**A**) HS1 or (**B**) HS1-M7A were cultured in SCE-LEU media for 15 hours with the indicated concentrations of the heme biosynthesis inhibitor succinylacetone (SA) and EGFP:mKATE2 fluorescence ratios were recorded. (**C-D**) *hem1*Δ cells expressing (**C**) HS1 or (**D**) HS1-M7A were cultured in SCE-LEU media for 15 hours with the indicated concentrations of 5-aminolevulinic acid (5-ALA) and EGFP:mKATE2 fluorescence ratios were recorded. The EGFP (ex. 488, em. 510) to mKATE2 (ex. 588, em. 620 nm) fluorescence ratio was recorded by a plate reader using 100 µL of $6x10^7$ cell/mL in PBS buffer. (**E**) Total heme content of WT or *hem1*Δ cells grown with 500 µM SA or 1.5 mM (200 µg/mL) 5-ALA, respectively, as determined by HPLC. All data represent the mean ± SD of triplicate cultures.

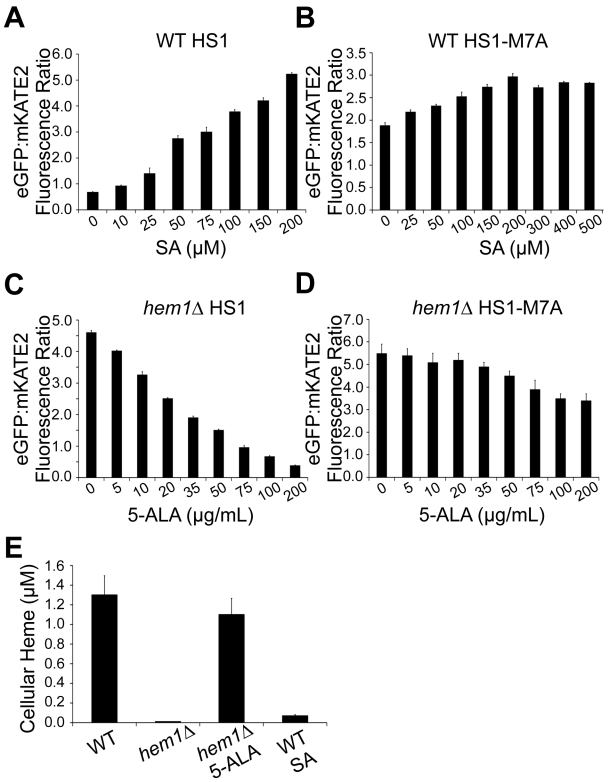

Figure S7. Heme-dependence of EGFP:mKATE2 fluorescence ratios of heme binding mutants and various N- and C-terminal mKATE2-CG6 fusion proteins expressed in *hem1*Δ cells cultured with the indicated concentration of 5-aminolevulinic acid (5-ALA). Only mKATE2-$(GS)_1$-CG6 exhibits a heme dependent EGFP to mKATE2 fluorescence ratio. The EGFP (ex. 488, em. 510) to mKATE2 (ex. 588, em. 620 nm) fluorescence ratio was recorded by a plate reader from 100 µL of $6x10^7$ cell/mL in PBS buffer. The data represent the mean ± SD of triplicate cultures. Cells were cultured to mid-exponential phase in SCE-LEU media prior to analyses.

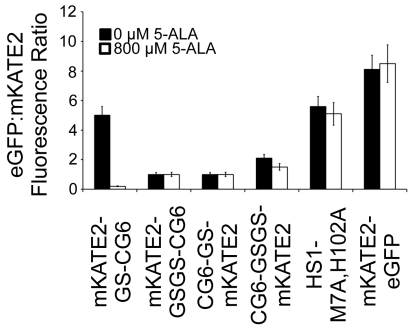

Figure S8. Expression of HS1-M7A does not perturb cell growth or heme regulated processes. (**A**) Representative quantitation of cellular HS1-M7A expression by immunoblotting using anti-GFP antibodies. Concentrations were determined by generating a standard curve using purified HS1-M7A. This analysis reveals that HS1-M7A driven by the GPD, TEF1, and ADH1 promoters are expressed at 5-10 nM, 2-4 nM, or .5-1 nM, respectively, in yeast cells. (**B**) Titration of HS1-M7A expression using GPD (strong), TEF1 (medium), or ADH1 (weak) promoters in WT or *hem1*Δ cells, as measured by mKATE2 fluorescence (ex. 588 nm, em. 620 nm), does not affect the sensor EGFP:mKATE2 ratio. This indicates that heme availability is unperturbed by sensor expression. HS1-M7A expression in WT cells does not affect (**C**) catalase activity, (**D**) total cellular heme levels, (**E**) growth, or (**F**) oxygen consumption. All cells were cultured to mid-exponential phase in SCE-LEU media prior to analyses.

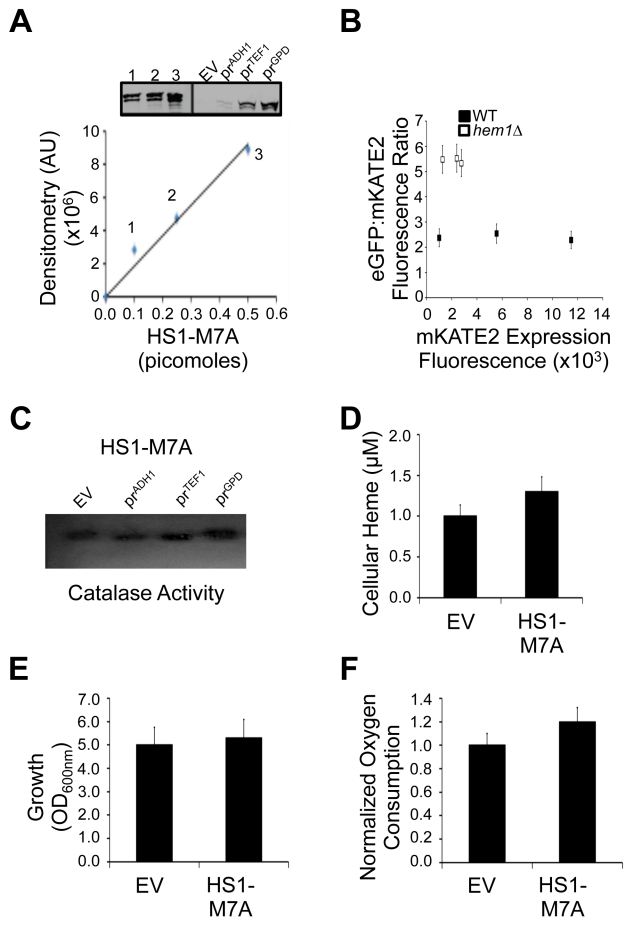

Figure S9. *In-situ* calibration of cytosolic HS1 and HS1-M7A. $6x10^7$ cells were harvested after 15 hours of growth and resuspended in 1 mL of PBS buffer. EGFP:mKATE2 fluorescence ratios were recorded by exciting EGFP (ex. 488) and mKATE2 (ex. 588) and collecting their emission at 510 nm and 620 nm, respectively. To calibrate the sensor and determine the ratio when they are 100% bound to heme (Heme Saturated), $6x10^7$ cells/mL were incubated for 30 minutes at 30 C in PBS buffer containing 1 mM ascorbate, 1 mg/mL digitonin, and 50 µM hemin chloride. After incubation, cells were washed of excess heme and fluorescence ratios were recorded as described for non-permeabilized cells. The data represent the mean ± SD of triplicate cultures. Cells were cultured to mid-exponential phase in SCE-LEU media prior to analyses.

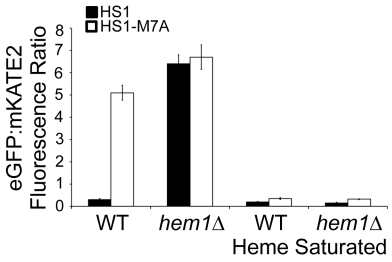

Figure S10. Simulation of the effect of labile heme oxidation state on the fractional saturation of HS1-M7A with heme. (**A-F**) Assuming various total *labile* heme concentrations, from 1-0.01 μM, the fraction of total sensor bound to ferric or ferrous heme is calculated as a function of the oxidation state of labile heme. Importantly, when the total labile heme pool is < 100 nM, the contribution of ferric heme binding is < 5%, indicating that HS1-M7A would be largely blind to the oxidized labile heme pool (if it existed). (**G**) A simulation depicting the relationship between the oxidation state of labile heme (y-axis) and the calculated labile heme pool (x-axis) for HS1-M7A that is 20-50% saturated with heme. All simulations were conducted using Hyperquad Simulation and Speciation HySS 2009 (40), assuming [HS1-M7A] = 10 nM, the concentration of HS1-M7A in cells (**Fig. S8A**), and K_D^{II} and K_D^{III} values of 25 nM and 1 μM (**Fig. S3**).

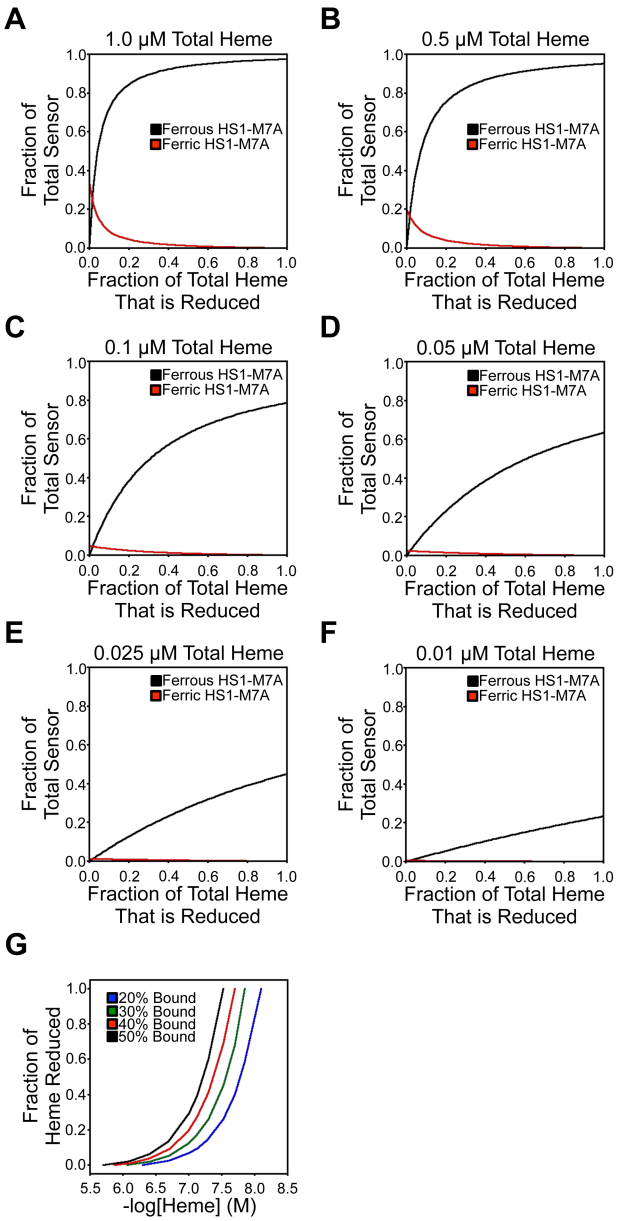

Figure S11. Variation in the tri-modal distribution of labile heme as measured by HS1-M7A. (**A-F**) Flow cytometry analysis of HS1-M7A EGFP:mKATE2 ratios in WT and *hem1*Δ cells in six independent trials. In each trial, cells were cultured in SCE-LEU media to mid-exponential phase before being subject to flow cytometry. (**F** and **G**) Replicate cell cultures indicate the low amount of variation in tri-modal distribution within one experimental trial (**F**), which is also indicated by the small deviation in the cell weighted average EGFP:mKATE2 ratio between the three replicates (**G**).

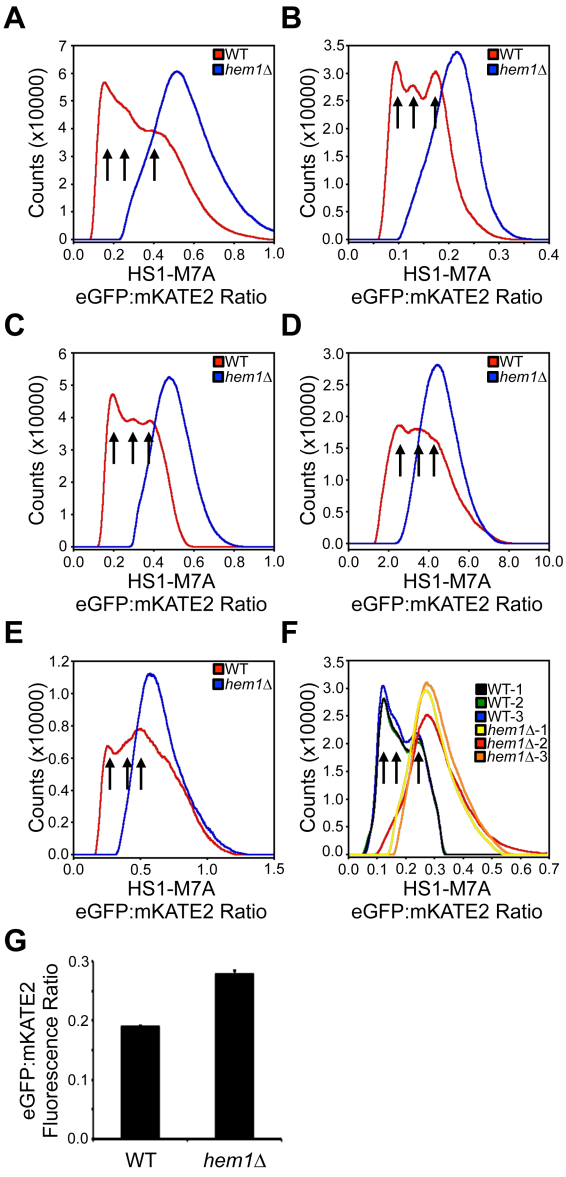

Figure S12. Variation in HS1 EGFP:mKATE2 fluorescence ratios as measured by flow cytometry. (**A-D**) Flow cytometry analysis of HS1 EGFP:mKATE2 ratios in WT and *hem1*Δ cells in four independent trials. In each trial, cells were cultured in SCE-LEU media to mid-exponential phase before being subject to flow cytometry.

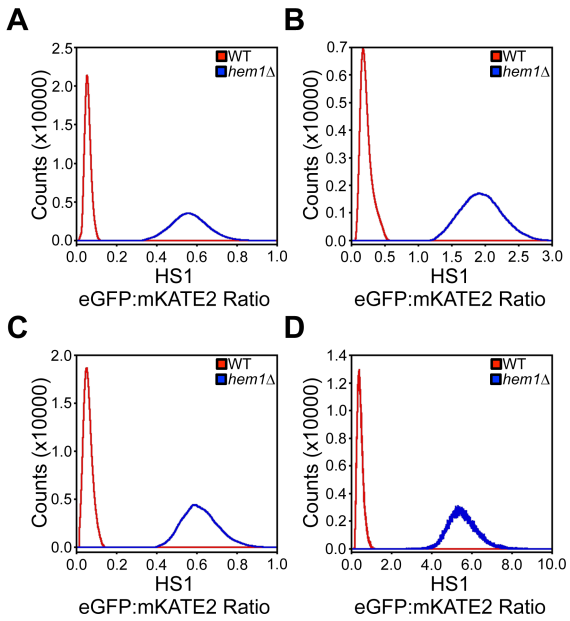

Figure S13. Titration of exogenous heme into total cell lysates from *hem1*Δ cells expressing HS1 or HS1-M7A targeted to the cytosol, mitochondria, or nucleus. $6x10^7$ cells were harvested after 15 hours of growth, resuspended in 0.2 mL of PBS buffer with 1 mM ascorbate, and lysed with zirconium oxide beads in a bead mill as described in the SI Methods. Lysates were incubated with the indicated concentrations of hemin chloride and EGFP:mKATE2 fluorescence ratios were recorded by exciting EGFP (ex. 488) and mKATE2 (ex. 588) and collecting their emission at 510 nm and 620 nm, respectively. The data represent the mean ± SD of triplicate cultures. Cells were cultured to mid-exponential phase in SCE-LEU media prior to analyses.

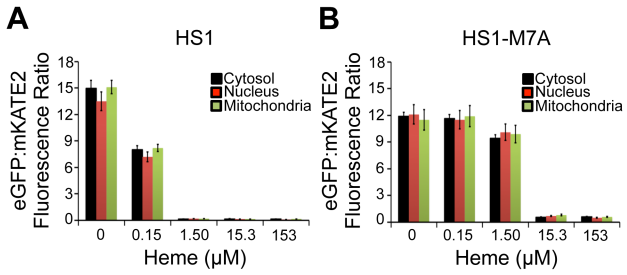

Figure S14. Mobilization of cytosolic heme by NO. (**A**) WT and *hem1*Δ cells expressing HS1-M7A were incubated with 5 μM NOC-7 and EGFP::mKATE2 fluorescence ratios were monitored. (**B**) WT cells expressing HS1-M7A were incubated with the indicated concentration of NOC-7 and EGFP::mKATE2 fluorescence ratios were monitored. (**C**) WT cells expressing HS1-M7A were incubated with the indicated concentration of NOC-7 and/or iodoacetamide (IAM) and EGFP::mKATE2 fluorescence ratios were monitored. (**D**) WT cells expressing HS1-M7A were incubated with the indicated concentration of NOC-7, diamide, H_2O_2 or paraquat (PQ) and EGFP:mKATE2 fluorescence ratios were monitored. Fluorimetry data represent the mean ± SD of triplicate cultures. Cells were cultured to mid-exponential phase in SCE-LEU media prior to analyses.

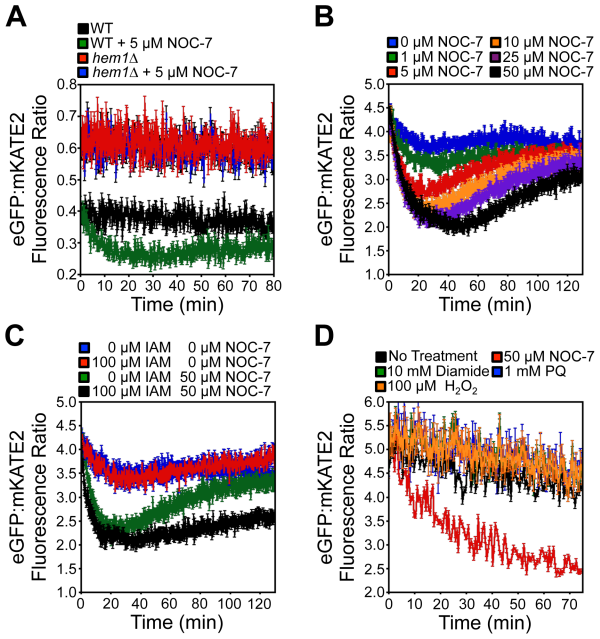

Figure S15. The effect of NOC-7 derived NO on purified HS1-M7A. 100 nM HS1-M7A was incubated in an aqueous buffered solution (20 mM PIPES, 100 mM NaCl, 1 mM ascorbate, pH 7.0) and the EGFP:mKATE2 fluorescence ratios were recorded over time as 0.3 equivalents of heme and 100 equivalents of NOC-7 was added at 0 and 10 minutes, respectively. Fluorimetry data represent the mean ± SD of duplicate samples.

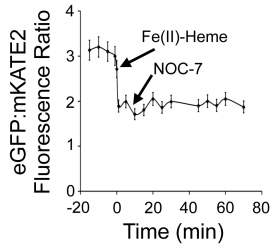

Figure S16. Effects of *TDH3* expression on total heme, catalase activity, and labile heme levels. (**A-C**) (**A**) Immunoblot analysis of GAPDH and SOD1 (loading control) in the indicated strains. (**B**) Total heme levels of the indicated strains as determined by HPLC. (**C**) In-gel activity assay for cytosolic catalase, Ctt1p, in the indicated strains. Cells were grown to mid-log phase in YPDE. Immunoblots and catalase activity are representative of two independent trials and the total heme levels represent the mean ± SD of triplicate cultures. (**D-E**) *TDH3* complementation of labile heme levels in *tdh3*Δ cells. (**D**) WT and *tdh3*Δ cells expressing empty vector (p416-GPD) or *TDH3* (p416-GPD-TDH3) and p415-ADH1-HS1-M7A were cultured in SCE-LEU-URA media for 15 hours and EGFP:mKATE2 fluorescence ratios were recorded. The fluorescence data was recorded as described for **Figure S6** and represent the mean ± SD of duplicate cultures. (**E**) Immunoblot analysis of GAPDH and SOD1 (loading control) in the strains from Panel D.

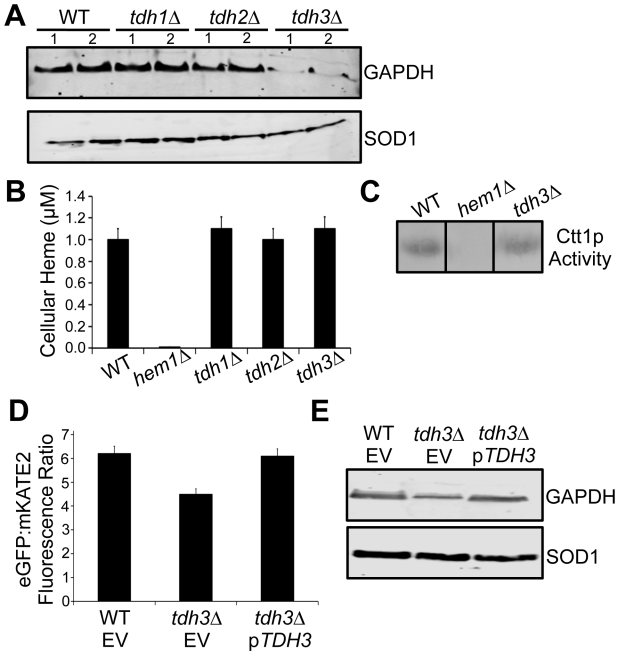

Figure S17. Validation of heme sensors in HEK293 and *E. coli* cells. Flow cytometry analysis of HEK293 cells transiently transfected with (**A**, **C**) HS1 or (**B**, **D**) HS1-M7A and cultured in regular media (heme replete) or heme deficient succinylacetone (SA) treated media (HD + SA). In panels **C** and **D**, cells were cultured in HD + SA media treated with the indicated concentrations of heme. (**E**) Laser scanning confocal microscopy of HEK293 cells expressing HS1 or HS1-M7A cultured in HD + SA media with or without 50 μM heme. (**F**) EGFP:mKATE2 fluorescence ratios of Δ*hemA E. coli* cells expressing HS1-M7A cultured in media with 5-aminolevulinic acid (5-ALA) or 90 min after shift to media lacking 5-ALA.

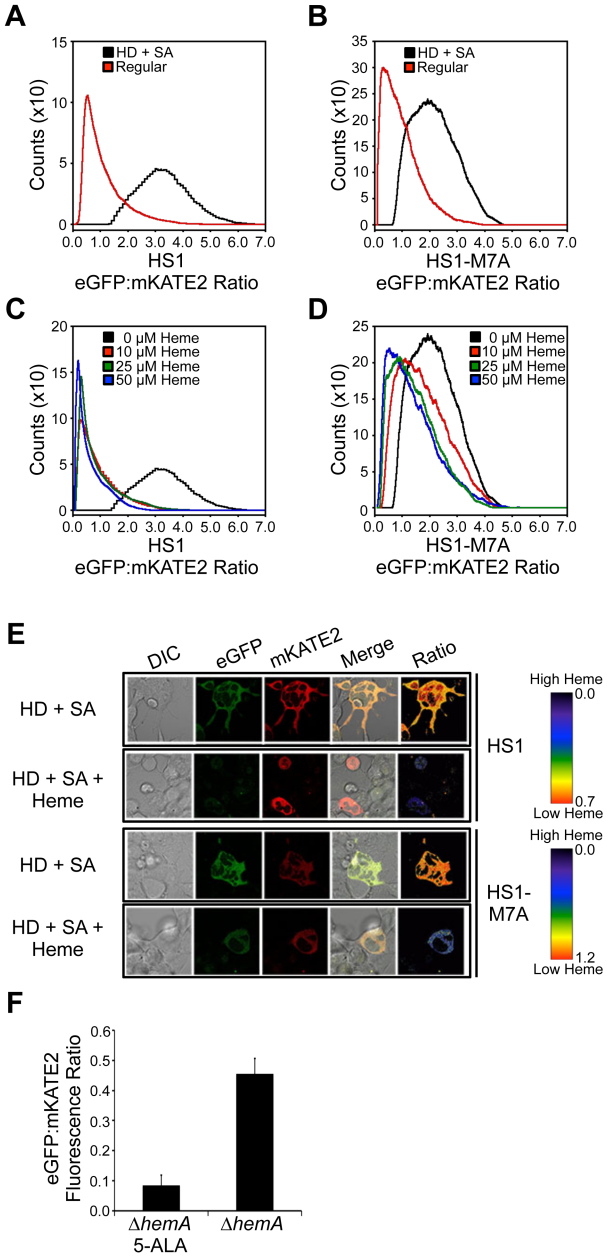

Figure S18. Mobilization of cytosolic heme by NO in WT and *tdh3*Δ cells. WT and *tdh3*Δ cells expressing p415-GPD-HS1-M7A were incubated with 10 μM NOC-7 and EGFP:mKATE2 fluorescence ratios were monitored. Fluorimetry data represent the mean ± SD of triplicate samples. Cells were cultured to mid-exponential phase in SCE-LEU media prior to analyses.

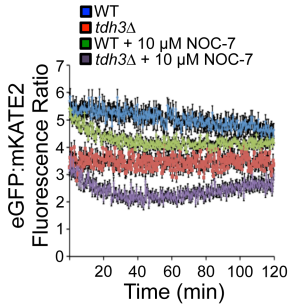

5. Supporting References

1. Gietz RD & Schiestl RH (1991) Applications of high efficiency lithium acetate trasformation of intact yeast cells using single-stranded nucleic acids as carrier. *Yeast* 7:253-263.
2. Ness F*, et al.* (1998) Sterol uptake in Saccharomyces cerevisiae heme auxotrophic mutants is affected by ergosterol and oleate but not by palmitoleate or by sterol esterification. *Journal of bacteriology* 180(7):1913-1919.
3. Wang L, Elliott M, & Elliott T (1999) Conditional stability of the HemA protein (glutamyl-tRNA reductase) regulates heme biosynthesis in Salmonella typhimurium. *Journal of bacteriology* 181(4):1211-1219.
4. Bertani G (2004) Lysogeny at mid-twentieth century: P1, P2, and other experimental systems. *Journal of bacteriology* 186(3):595-600.
5. Wu Y & Outten FW (2009) IscR controls iron-dependent biofilm formation in Escherichia coli by regulating type I fimbria expression. *Journal of bacteriology* 191(4):1248-1257.
6. Zhu Y, Hon T, Ye W, & Zhang L (2002) Heme deficiency interferes with the Ras-mitogen-activated protein kinase signaling pathway and expression of a subset of neuronal genes. *Cell Growth Differ* 13(9):431-439.
7. Vuletic I*, et al.* (2015) Establishment of an mKate2-Expressing Cell Line for Non-Invasive Real-Time Breast Cancer In Vivo Imaging. *Molecular imaging and biology : MIB : the official publication of the Academy of Molecular Imaging*.
8. Li D*, et al.* (2011) [Labeling of liver cancer cell for fluorescence imaging study by far-red fluorescence protein reporter gene mKate2]. *Zhonghua yi xue za zhi* 91(19):1344-1347.
9. Arpino JA*, et al.* (2012) Structural basis for efficient chromophore communication and energy transfer in a constructed didomain protein scaffold. *Journal of the American Chemical Society* 134(33):13632-13640.
10. Mumberg D, Muller R, & Funk M (1995) Yeast vectors for the controlled expression of heterologous proteins in different genetic backgrounds. *Gene* 156(1):119-122.
11. Hu J, Dong L, & Outten CE (2008) The redox environment in the mitochondrial intermembrane space is maintained separately from the cytosol and matrix. *The Journal of biological chemistry* 283(43):29126-29134.
12. Tsang C. K. L, Y., Thomas, J., Zhang. Y., Zheng X. F. (2014) Superoxide dismutase 1 acts as a nuclear transcription factor to regulate oxidative stress resistance. *Nature communications* 5:3446.
13. Sikorski RS & Hieter P (1989) A system of shuttle vectors and yeast host strains designed for efficient manipulation of DNA in *Saccharomyces ceresiviae*. *Genetics* 122:19-27.
14. Bradford M (1976) A Rapid and Sensitive Method for the Quantitation of Microgram Quantities of Protein Utilizing the Principle of Protein-Dye Binding. *Analytical Biochemistry* 72(1-2):248-254.
15. Hill SE, Donegan RK, & Lieberman RL (2014) The glaucoma-associated olfactomedin domain of myocilin forms polymorphic fibrils that are constrained by

partial unfolding and peptide sequence. *Journal of molecular biology* 426(4):921-935.
16. Schneider CA, Rasband WS, & Eliceiri KW (2012) NIH Image to ImageJ: 25 years of image analysis. *Nature methods* 9(7):671-675.
17. Ruzin SE (1999) *Plant microtechnique and microscopy* (Oxford University Press, New York) pp xi, 322 p.
18. Zhuang J*, et al.* (2006) Evaluating the roles of the heme a side chains in cytochrome c oxidase using designed heme proteins. *Biochemistry* 45(41):12530-12538.
19. Thompson AM*, et al.* (2007) Measurement of the heme affinity for yeast dap1p, and its importance in cellular function. *Biochemistry* 46(50):14629-14637.
20. Reddi AR, Reedy CJ, Mui S, & Gibney BR (2007) Thermodynamic investigation into the mechanisms of proton-coupled electron transfer events in heme protein maquettes. *Biochemistry* 46(1):291-305.
21. Reddi AR, Guzman TR, Breece RM, Tierney DL, & Gibney BR (2007) Deducing the energetic cost of protein folding in zinc finger proteins using designed metallopeptides. *Journal of the American Chemical Society* 129(42):12815-12827.
22. Reddi AR, Pawlowska M, & Gibney BR (2015) Evaluation of the Intrinsic Zn(II) Affinity of a Cys3His1 Site in the Absence of Protein Folding Effects. *Inorganic chemistry* 54(12):5942-5948.
23. Reddi AR & Gibney BR (2007) Role of protons in the thermodynamic contribution of a Zn(II)-Cys4 site toward metalloprotein stability. *Biochemistry* 46(12):3745-3758.
24. Petros AK, Reddi AR, Kennedy ML, Hyslop AG, & Gibney BR (2006) Femtomolar Zn(II) affinity in a peptide-based ligand designed to model thiolate-rich metalloprotein active sites. *Inorganic chemistry* 45(25):9941-9958.
25. Song Y*, et al.* (2015) A Genetically Encoded FRET Sensor for Intracellular Heme. *ACS chemical biology* 10(7):1610-1615.
26. Grynkiewicz G, Poenie M, & Tsien RY (1985) A new generation of Ca2+ indicators with greatly improved fluorescence properties. *The Journal of biological chemistry* 260(6):3440-3450.
27. Ebert PS, Hess RA, Frykholm BC, & Tschudy DP (1979) Succinylacetone, a potent inhibitor of heme biosynthesis: effect on cell growth, heme content and delta-aminolevulinic acid dehydratase activity of malignant murine erythroleukemia cells. *Biochemical and biophysical research communications* 88(4):1382-1390.
28. Reddi AR & Culotta VC (2013) SOD1 integrates signals from oxygen and glucose to repress respiration. *Cell* 152(1-2):224-235.
29. Baureder M & Hederstedt L (2012) Genes important for catalase activity in Enterococcus faecalis. *PloS one* 7(5):e36725.
30. Woods JS & Simmonds PL (2001) HPLC methods for analysis of porphyrins in biological media. *Current protocols in toxicology / editorial board, Mahin D. Maines* Chapter 8:Unit 8 9.

31. Reddi AR & Culotta VC (2011) Regulation of Manganese Antioxidants by Nutrient Sensing Pathways in Saccharomyces cerevisiae. *Genetics* 189:1261-1270.
32. Takeda S, Kamiya N, Arai R, & Nagamune T (2001) Design of an artificial light-harvesting unit by protein engineering: cytochrome b(562)-green fluorescent Protein chimera. *Biochemical and biophysical research communications* 289(1):299-304.
33. Hargrove MS, Barrick D, & Olson JS (1996) The association rate constant for heme binding to globin is independent of protein structure. *Biochemistry* 35(35):11293-11299.
34. Morgan WT, Liem HH, Sutor RP, & Muller-Ebergard U (1976) Transfer of heme from heme-albumin to hemopexin. *Biochimica et biophysica acta* 444(2):435-445.
35. Koga S*, et al.* (2013) Development of a heme sensor using fluorescently labeled heme oxygenase-1. *Analytical biochemistry* 433(1):2-9.
36. Fleischhacker AS*, et al.* (2015) The C-terminal heme regulatory motifs of heme oxygenase-2 are redox-regulated heme binding sites. *Biochemistry* 54(17):2709-2718.
37. Gupta N & Ragsdale SW (2011) Thiol-disulfide redox dependence of heme binding and heme ligand switching in nuclear hormone receptor rev-erb{beta}. *The Journal of biological chemistry* 286(6):4392-4403.
38. Kamal JK & Behere DV (2005) Binding of heme to human serum albumin: steady-state fluorescence, circular dichroism and optical difference spectroscopic studies. *Indian J Biochem Biophys* 42(1):7-12.
39. Zhang L & Guarente L (1995) Heme binds to a short sequence that serves a regulatory function in diverse proteins. *The EMBO journal* 14(2):313-320.
40. Gans P, Sabatini A, & Vacca A (1996) Investigation of equilibria in solution. Determination of equilibrium constants with the HYPERQUAD suite of programs. *Talanta* 43(10):1739-1753.